

Quartz enhanced laser photoacoustic sensors for remote sensing

Ramesh C. Sharma*, Deepak Kumar,
Neha Bhardwaj and Anil K. Maini

Laser Science and Technology Centre,
Defence Research and Development Organization, Metcalfe House,
Delhi 110 054, India

We report an active spectral sensor for chlorophyll detection based on quartz crystal tuning fork detector. The sensors use modulated diode laser radiations that can be differentiated from ambient background radiations by the detector. Experimentally, electrical and optical parameters of quartz crystal tuning fork detector (QCTF) were studied. Linear dependence of optical power to the generated electrical signals of QCTF detector was derived by measurements at different optical powers and wavelengths. We report here Quartz Enhanced Laser Photoacoustic signal of chlorophyll traces dissolved in water and adsorbed on surfaces, using 532 nm and 635 nm wavelength lasers from a standoff distance of up to 25 m. With the availability of high-power tunable diode laser, the technique offers a wide range of applicability for point and standoff sensing.

Keywords: Chlorophyll detection, diode laser, spectral sensor, quartz crystal tuning fork.

QUARTZ Enhanced Laser Photoacoustic spectroscopy (QE-LPAS) technology is a promising powerful standoff technique for environmental sciences, medical sciences and homeland security in defence¹⁻³. The QE-LPAS technique has shown detection capability of a variety of chemicals at parts per billion (ppb) level concentration, with very low false alarm rates^{4,5}. Conventional LPAS systems have been used to study various hazardous chemicals and corrosive vapours^{6,7}. QE-LPAS and photothermal spectroscopy-based systems have been used for environmental monitoring and homeland security⁸⁻¹¹. Gas sensing based on the QE-LPAS technique has been developed with very high sensitivity¹². Fibre-coupled quantum cascade laser (QCL) emitting in mid-infrared wavelength-based QE-LPAS sensor has been studied for parts per trillion (ppt) level detection of SF₆ (sulphur hexafluoride) (ref. 13).

The aim of present work is to demonstrate QE-LPAS active standoff signal of trace chlorophyll in water and that adsorbed on the surface of cloth and wood. We have studied the electrical and optical properties of quartz crystal tuning fork (QCTF) detector. The modulated diode pumped solid state laser (DPSSL) at 532 nm (low absorption band of chlorophyll) and diode lasers at 635 nm (high absorption band of chlorophyll) are two

incident sources used to study the absorption of chlorophyll samples in traces. Spectral absorption and reflection due to chlorophyll is associated with plant physiological characteristics, such that plant stress results in an increase in visible reflectance at 400–700 nm wavelength and a decrease in near-infrared (NIR) reflectance at 700–1300 nm wavelength. Differences in spectral reflectance in the visible and NIR wavelengths are used to calculate a normalized difference vegetation index (NDVI) and have been used for many ground-based mapping applications utilizing active spectral sensors¹⁴. NDVI can also be determined by this method using NIR and visible laser diodes.

A commercially available QCTF detector (Citizen Model CFS308 of frequency 32.8 kHz) having dimensions ~ 1.5 mm × 0.25 mm × 6 mm is used. A small periodic force generated due to modulated light incident on the prongs of QCTF at a repetition rate matching its resonance frequency (f_0) drives it into oscillation. Due to the piezoelectric properties of the quartz material, this force gives rise to a periodic electrical current signal proportional to the deflection of the prongs. Since the modulation of the driving force is done at the resonance frequency of the tuning fork, a significant enhancement in signal is achieved. The resonance frequency and optical response is to be determined experimentally before measurements.

The QCTF detector was studied for its Q value, resonant frequency f_0 and its electrical equivalent, R , L and C . The electrical characteristics are studied using a trans-impedance circuit (Figure 1 a) having QCTF detector at its input. A voltage of 100 mV p-p (peak to peak) is applied to the detector by varying input modulation frequencies. Input frequency to the QCTF detector versus

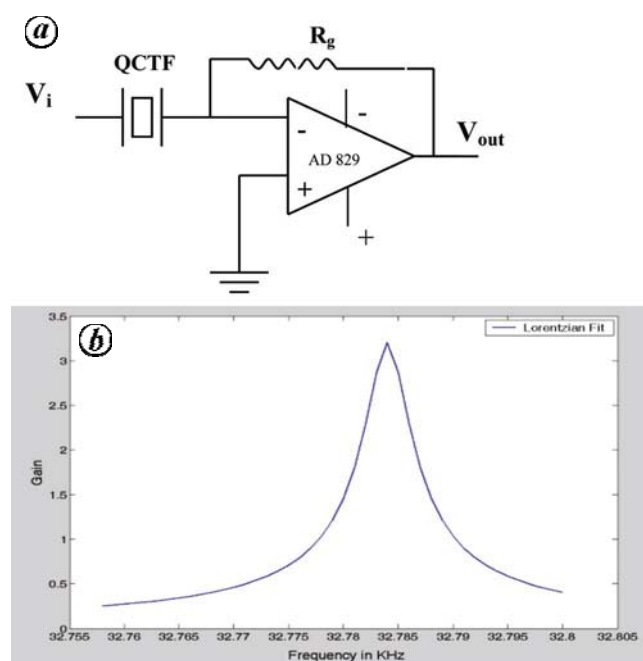


Figure 1. a, Trans-impedance amplifier circuit. b, Gain versus input frequency of QCTF.

*For correspondence. (e-mail: rameshsharma@lastec.drdo.in)

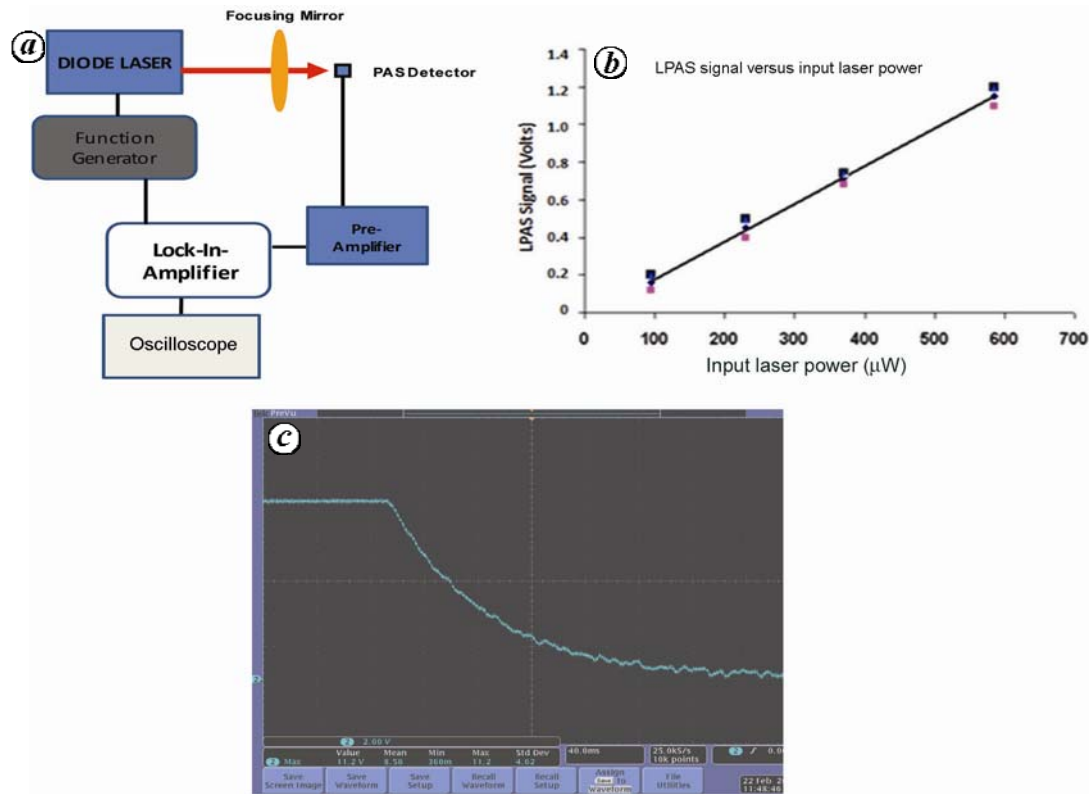


Figure 2. *a*, Optical set-up for QCTF detector. *b*, Optical characterization of QCTF detector. *c*, Detector voltage versus time (ms) (oscilloscope trace).

signal is plotted in Figure 1 *b*. The peak position shows the resonant frequency (f_0), Δf (~ 4 Hz) the full width at half maxima (FWHM), and the ratio ($f_0/\Delta f$) gives the Q value. The following parameters are determined: $Q \sim 8000$ and resonant frequency $f_0 = 32.784$ kHz.

Figure 2 *a* shows the experimental set-up of optical characterization of QCTF detector. Both the lasers of wavelength 635 nm and 532 nm were used. The lasers were modulated to the resonant frequency of QCTF by a function generator. Rectangular driving pulses with varying duty cycle were applied to select different laser power levels. A focusing lens of 5.0 cm aperture and 40 cm focal length was used to focus the beam on the QCTF detector. A pre-amplifier with a trans-impedance circuit based on AD829 IC having feedback resistor of 1 M Ω is used to feed the signal to lock-in amplifier (Stanford Model SRS-830). Sine wave signal of modulating frequency of diode laser is given as reference signal to lock-in-amplifier. The time constant of lock-in amplifier was taken as 10–100 ms. Sensitivity of lock-in amplifier was changed according to laser power levels. Signal amplified by lock-in amplifier is fed to digital storage oscilloscope (Tektronics DPO 3054) for measurements.

LPAS signal measured at oscilloscope (V) versus incident power (μ W) of diode laser on the QCTF detector is plotted in Figure 2 *b*. Signal versus input power data are linear-fitted ($y = mx + c$), the slope value obtained is

0.0021. Experimentally it was observed that there is a linear dependence between the input laser power and the output voltage signal. Decay time was obtained experimentally by blocking the laser beam and recording the signal voltage trace as shown in Figure 2 *c*. Decay time (τ) = time at (1/e) ($e = 2.718$) times peak voltage is measured as 80 ms.

$$\tau = \frac{Q}{\pi f_0}, \tag{1}$$

where τ is the decay time, implies Q is the decay time. $Q = \tau \pi f$, implies $Q = 0.080 \cdot \pi \cdot 3784 = 8240$. Q value calculated by optical set-up is 8240, which is in good agreement with that measured from electrical set-up.

For the standoff detection, the detector parameters like noise current, responsivity, detectivity (D^*) and noise equivalent power (NEP) need to be evaluated. The current (I) per deflection (X_L) of the tuning fork is given by¹⁴

$$\frac{I}{X_L} = 2\pi f_0 \cdot 3 d_{12} E \frac{TW}{L}, \tag{2}$$

where T is thickness, W width, L length of the tuning fork; the piezoelectric coupling constant, $d_{12} = 2.31 \times 10^{-12}$ Coulomb/Newton; Young's modulus $E = 7.87 \times 10^{10}$ N/m² for quartz and resonant frequency $f_0 = 32.80$ kHz, current

per deflection of 4.5 A/m is theoretically determined for the QCTF. The mean square amplitude of the tuning fork fine vibration in thermal equilibrium is calculated from the equipartition theorem

$$\frac{1}{2} k \langle x_{\text{rms}} \rangle^2 = \frac{1}{2} k_B T, \quad (3)$$

where k is the spring constant, x_{rms} the root mean deflection, k_B the Boltzmann constant and T the absolute temperature. At room temperature ($T = 300$ K), $x_{\text{rms}} = 2.94$ pm, the noise current spectral density is the current generated ($I = I_N$) per unit x_{rms} and per unit bandwidth equals to $I_N = 1.32 \times 10^{-11}$ amp/Hz^{1/2}, as derived from eq. (3). The set-up in Figure 2 a is used to evaluate experimentally the responsivity of the QCTF detector. Figure 2 b is the plot of QE-LPAS signal versus incident laser power on the QCTF detector. Experimentally, a responsivity $R = 2 \times 10^{-3}$ amp/W at the output of trans-impedance amplifier with a feedback resistance of 1 M Ω is measured, which results in NEP.

$$\text{NEP} = \frac{I_N}{R(\text{responsivity})} = 6.6 \text{ nW/Hz}^{1/2}. \quad (4)$$

$$\begin{aligned} \text{Detectivity } (D^*) &= \sqrt{A}/\text{NEP} \\ &= 3.36 \times 10^6 \text{ cm Hz}^{1/2}/\text{W}. \end{aligned} \quad (5)$$

For the sensing area, the maximum circular spot fitting on the lateral surface of the tuning fork with a diameter of 250 μm has been used. A (250 ± 10) micron variation of circular focus spot size on the tuning fork will result in a $\pm 5\%$ variation in the detectivity of the QCTF detector. The QCTF detector has shown response to optical radiations: UV to terahertz radiations. We have checked the optical response of QCTF at 532 nm, 635 nm and also mid-IR band 7.1–12 μm using quantum cascade laser (QCL). Replacing the diode laser by QCL in Figure 2 a, similar response of the detector as plotted in Figure 2 b is observed for all the wavelengths.

Standoff laser photoacoustic signal measurement of chlorophyll was carried out from a distance of up to 25 m. Chlorophyll paste derived from tree leaf was applied on cloth surface and wooden block placed at a distance of 10.0 and 25.0 m respectively from the detector using the laser wavelengths 532 and 635 nm. Diode laser wavelength at 632 nm corresponds to high absorption band of chlorophyll and 532 nm to the very low absorption band of chlorophyll. The 532 nm wavelength is used for calibration/baseline purpose. Modulated laser beams were transmitted onto the target. Diode laser beam is modulated at the frequency ~ 32.80 kHz using the function generator for a duty cycle of 25% (power 10 mW for both lasers). Incident radiation is absorbed by the chlorophyll paste at the surface of different targets and rest of

the laser radiations, backscattered/reflected towards the target, are collected by a receiver mirror and focused on the QCTF detector. The laser photoacoustic signal is processed through the electronics set-up as shown in Figure 3 a.

The photoacoustic signal for the adsorbed surfaces is shown in Figure 3 b. The normalized LPAS signal versus concentration ($\mu\text{g}/\text{cm}^2$) from chlorophyll pasted on wood and cloth (10 and 25 m) is plotted in Figure 3 b. Normalized photoacoustic signal is calculated by subtracting the 635 nm signal from the 532 nm signal. As the concentration increases, the normalized QE-LPAS signal increases linearly.

We also recorded QE-LPAS signal of chlorophyll dissolved in water in quartz cuvette placed at a distance of 25 m having concentration ~ 50 ppm with diffused aluminum plate in the background. The normalized photoacoustic signal for different background surfaces (wood and cloth) is calculated by subtracting the LPAS signal obtained using 635 nm from LPAS signal obtained using 532 nm, i.e. (normalized photoacoustic signal = LPAS signal chlorophyll using 532 nm – LPAS signal chlorophyll using 635 nm). We have also measured photoacoustic signal for chlorophyll concentration of 100 ng/cm² on diffused wood surface. A change of detector characteristics results in $\pm 5\%$ variation of detection concentration. The normalized LPAS signal increases with increasing concentration of adsorbed chlorophyll on the surface (Figure 3 b).

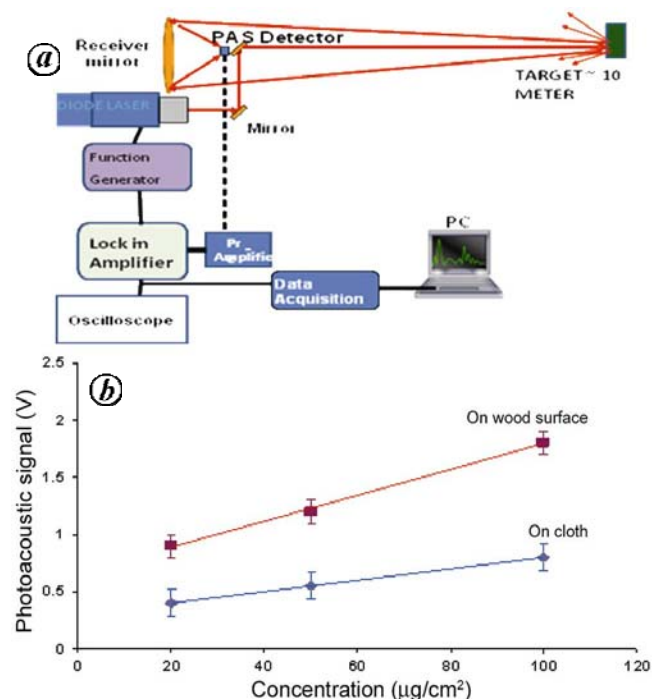


Figure 3. a, Standoff QE-LPAS set-up. b, Standoff normalized LPAS signal versus concentration of chlorophyll for target materials: wood and cloth.

$$\text{NDVI} = \frac{\rho_{\text{NIR}} - \rho_{\text{VIS}}}{\rho_{\text{NIR}} + \rho_{\text{VIS}}}$$

can also be determined by this method using NIR and visible laser diodes.

The experimental work has been carried out for stand-off LPAS signal using QCTF detector. Resonant frequency (f) and quality factor (Q) of QCTF were evaluated using both electrical and optical experimental set-ups. A linear dependence of optical power (W) to electrical LPAS signal (V) is derived by measurement at different optical power levels. Ambient solar or optical radiation sources do not introduce any noise in QE LPAS signal, which results into a high signal-to-noise ratio. The technique only works at the resonant frequency of the QCTF detector. In the experiment, standoff laser photoacoustic sensor is successfully demonstrated for detection of adsorbing chlorophyll traces on surfaces like diffused wood and cotton cloth. The normalized LPAS signal increases with increasing concentration of adsorbed chlorophyll on the surface; wood and cloth. Q value calculated by the optical set-up is 8240, which is in good agreement with that measured (8000) from electrical set-up. The very low cost and very wide spectral response without any cooling requirement has made the QCTF detector a promising tool for wide spectral band from UV to terahertz. In future, QE-LPAS-based systems can be used in the environmental sensing for organic matter monitoring, plant disease studies, photosynthesis, oil pollution, hazardous chemicals and homeland security applications.

1. Van Neste, C. W., Senesac, L. R. and Thundat, T., Standoff photoacoustic spectroscopy. *Appl. Phys. Lett.*, 2008, **92**, 234102–234106.
2. Gurton, K., Felton, M. and Tober, R., Real-time detection of chemical warfare agents using multi-wavelength photoacoustics, ARL-TR-4782, US Army Research Lab, April 2009.
3. Van Neste, C. W., Senesac, L. R. and Thundat, T., Standoff spectroscopy of surface adsorbed chemicals. *Anal. Chem.*, 2009, **81**, 1952–1956.
4. Bauer, C. *et al.*, A mid-infrared QEPAS sensor device for TATP detection. *J. Phys.: Conf. Ser.*, 2009, **157**, 012002–012005.
5. Pushkarsky, M. B., Dunayevskiy, I. G., Prasanna, M., Tsekoun, A. G., Go, R. and Patel, C. K. N., High-sensitivity detection of TNT, *Proc. Natl. Acad. Sci. USA*, 2006, **103**, 19630–19632.
6. Prasad, R. L., Prasad, R., Bhar, G. C. and Thakur, S. N., Photoacoustic spectra and modes of vibration of TNT and RDX at CO₂ laser wavelengths. *Spectrochim. Acta A*, 2002, **58**, 3093–3095.
7. Sharma, R. C., Thakur, S. N. and Lin, K. C., A³ $\pi_{1u} \leftarrow X1\Sigma_g^+$ laser photoacoustic spectroscopy of Br₂ vapor in the extreme red wavelength region 665–720 nm. *Spectrochim. Acta Part A*, 2004, **6**, 1889–1893.
8. Mukherjee, A., Von der Porten, S., Kumar, C. and Patel, C. K. N., Standoff detection of explosive substances at distances of up to 150 m. *Appl. Opt.*, 2010, **49**, 2072–2075.
9. Pohlkötter, A., Köhring, M., Willer, U. and Schade, W., Detection of molecular oxygen at low concentrations using quartz enhanced photoacoustic spectroscopy. *Sensors*, 2010, **10**, 8466–8477.
10. Kostereva, A. A. and Tittel, F. K., Applications of quartz tuning forks in spectroscopic gas sensing. *Rev. Sci. Instrum.*, 2005, **76**, 043105–043107.

11. Furstenberg, R. *et al.*, Stand-off detection of trace explosives by infrared photo-thermal spectroscopy. *IEEE*, 2009, **978**, 465–471.
12. Jahjah, M., Belahsene, S., Nähle, L., Fischer, M., Koeth, J., Rouillard, Y. and Vicet, A., Quartz enhanced photoacoustic spectroscopy with a 3.38 μm antimonide distributed feedback laser. *Opt. Lett.*, 2012, **37**, 2502.
13. Spagnolo, V., Patimisco, P., Borri, S., Scamarcio, G., Bernacki, B. E. and Kriesel, J., Part-per-trillion level SF₆ detection using a quartz enhanced photoacoustic spectroscopy-based sensor with single-mode fiber-coupled quantum cascade laser excitation. *Opt. Lett.*, 2012, **37**, 4461.
14. Pohlkötter, A., Willer, U., Bauer, C. and Schade, W., Resonant tuning fork detector for electromagnetic radiation. *Appl. Opt.*, 2009, **48**, B119–B125.

ACKNOWLEDGEMENTS. We thank Prof. Thomas Thundat and Dr C. W. Van Neste, University of Alberta, Canada for discussions on the standoff QE-LPAS technology.

Received 30 January 2013; revised accepted 23 April 2013

Tectonics and climate interplay: exhumation patterns of the Dhauladhar Range, Northwest Himalaya

Vikas Adlakha¹, R. C. Patel^{1,*}, Nand Lal¹, Y. P. Mehta², A. K. Jain³ and Ashok Kumar⁴

¹Department of Geophysics, Kurukshetra University, Kurukshetra 136 119, India

²S.A. Jain College, Ambala City 134 003, India

³Central Building Research Institute, Roorkee 247 667, India

⁴D.A.V. College, Ambala City 134 003, India

New apatite and zircon fission-track ages from the Dalhousie Granite exposed along Dhauladhar Range, Northwest Himalaya extend from 2.9 ± 0.2 to 4.4 ± 1.0 Ma and 10.4 ± 1.4 to 21.1 ± 2.2 Ma respectively. One-dimensional thermal modelling of the data suggests slow exhumation during Middle to Late Miocene, followed by acceleration during Plio-Pleistocene. The activity along the Panjal Thrust (PT)/Main Central Thrust (MCT) in this region ceased at ~ 15 Ma, while tectonic activity along the Main Boundary Thrust (MBT) started prior to ~ 10 Ma. Tilting of topography due to activation of MBT controls the exhumation pattern of Dalhousie Granite during Middle to Late Miocene. Correlation among structure, topographic pattern and thermochronometric ages indicates interplay between tectonics and erosion-controlled exhumation along the mountain front. The fast exhumation rates since Pliocene are synchronous

*For correspondence. (e-mail: patelramesh_chandra@rediffmail.com)